Using liquid crystals for *in situ* optical mapping of interfacial mobility and surfactant concentrations at flowing aqueous-oil interfaces

*Sangchul Roh, Michael Tsuei, and Nicholas L. Abbott**

Smith School of Chemical and Biomolecular Engineering, Cornell University, Ithaca, NY 14853, USA.

KEYWORDS. Marangoni stress, Liquid crystals, Non-equilibrium, Oil-water interfaces, Interfacial mobility, Surfactants

ABSTRACT: Flow-induced states of fluid interfaces decorated with amphiphiles underlie phenomena such as emulsification, foaming and spreading. While past studies have shown that interfacial mass transfer, the kinetics of surfactant adsorption and desorption, interfacial mobility and surfactant reorganization regulate the dynamic properties of surfactant-laden interfaces, few simple methods permit simultaneous monitoring of this interplay. Here we explore the optical responses of micrometer-thick films of oils (4-cyano-4′-pentylbiphenyl, 5CB) with liquid crystalline order in contact with flowing aqueous phases of soluble (e.g., sodium dodecyl sulfate (SDS)) or insoluble (e.g., 1,2-dilauroyl-sn-glycero-3-phosphocholine (DLPC)) amphiphiles. We observe the onset of flow of 0.5 mM SDS solutions within a millifluidic channel (area-average

velocity of 200 mm/s) to transform a liquid crystal (LC) film with an alignment along the interface normal into a bright birefringent state (average LC tilt angle of 30°), consistent with an initially mobile interface that shears and thus tilts the LC along the flow direction. Subsequently, we observed the LC film to evolve to a steady state (over ~10 s) with position-dependent optical retardance controlled by gradients in surfactant concentration and thus Marangoni stresses. For 0.5 mM SDS solutions, by using particle tracking and a simple hydrodynamic model, we reveal that the dominate role of the flow-induced interfacial surfactant concentration gradient is to change the mobility of the interface (and thus shear rate of LC) and not to change the easy axis (equilibrium orientation) or anchoring energy (orientation-dependent interfacial energy) of the LC. At lower surfactant concentrations (0.015 mM SDS), however, we show that the LC directly maps flow-induced interfacial surfactant concentration gradients via a change in the local easy axis of the LC. When combined with additional measurements obtained with simple salts and insoluble amphiphiles, these results hint that LC oils may offer the basis of general and facile methods that permit mapping of both interfacial mobility and surfactant distributions at flowing interfaces.

INTRODUCTION

Understanding the non-equilibrium distributions of amphiphiles at complex fluid interfaces undergoing flow is fundamental to a wide range of applications of amphiphiles, ranging from foods and personal care products to oil recovery.[1–8] Under shear flow, amphiphiles at interfaces are advected in the flow direction.[1,6,9–11] Any resulting spatial variation of the interfacial concentration of amphiphiles can trigger a gradient in surface pressure (Marangoni stresses), thereby counterbalancing hydrodynamic shear stresses and decreasing the mobility (motion) of the

interface.[7,12–14] Marangoni stresses induced by flow at interfaces are also strongly influenced by adsorption and desorption kinetics of amphiphiles, as adsorption/desorption diminishes the magnitude of the spatial gradient in interfacial amphiphile concentration.[15–18] Direct mapping of the surface concentration of amphiphiles has been performed using fluorescent amphiphiles, but this approach requires chemical modification of amphiphiles, which is laborious and potentially alters their adsorption and desorption characteristics.[9,19,20] Because direct mapping of the excess concentration of unmodified amphiphiles at flowing interfaces is challenging, studies of amphiphiles at mobile interfaces under shear have typically involved direct measurement of interfacial velocities and/or interface shapes, with Marangoni stresses and interfacial distributions of amphiphiles inferred from transport models of advection and diffusion at the interfaces.[8,12,14,21] Examples of such studies include measurement of the rise velocity of air bubbles in liquids or tracer particle displacement at sheared interfaces.[1,14,21] In the study reported herein, we explore the use of liquid crystalline oils as the basis of fresh approaches for optical imaging of the mobility and distribution of amphiphiles at flowing interfaces.

The liquid crystals (LCs) used in our study are oils within which the constituent molecules exhibit long-range orientational order (so-called nematic LCs).[22–24] The long-range order leads to several key properties that we exploit in our study, including optical anisotropy, elasticity, surface-induced orientational anchoring, and anisotropic viscosity. Below, we briefly introduce each of these properties, and explain how we harness them to enable our study of the mobility and distribution of amphiphiles at oil-water interfaces under shear.

We exploit the orientation-dependent optical properties of LCs to report spatial and temporal variations in LC orientations that reflect changes in interfacial mobility and the distribution of amphiphiles adsorbed at LC-aqueous interfaces. For nematic phases of 4-cyano-

4′-pentylbiphenyl (5CB, Fig. 1a) at 25°C, as used in our study, the orientation-dependent refractive indices range from 1.71 (so-called extraordinary index) to 1.53 (ordinary refractive index). This anisotropy generates optical retardance values $r = \Delta n\, d$, where Δn is birefringence and d is the LC thickness,[20,24] of up to 3600 nm for a 20 μm-thick LC film: Changes in the orientations of films of nematic 5CB induced by shear stresses can trigger large and easily quantified changes in the optical retardance and transmission of light through the LC.

The LC films used in the experiments reported in this paper are, prior to introduction of slow, uniformly oriented. When uniformly oriented LC thin films are reoriented by interfacial hydrodynamic shear stresses or the arrival interfacial adsorbates, the change in orientation is typically opposed by a rise in elastic free energy as the LC is strained away from the intial state. The simplest description of the elastic energy stored in a strained LC can be written in terms of splay, bend, twist, and saddle-splay modes of deformation (the so-called Frank-Oseen elastic energy).[22,24] For LC films that vary in tilt angle across the film thickness (defined as a z direction), the elastic free energy density can be expressed as $f_{FO}=f_{FO}(\theta,\theta')$, where θ is the tilt angle of the LC and θ′ is the first order derivative of LC tilt angle. Below we use this simple description of the elastic energy to describe the response of LC films to flowing surfactant solutions.

The free energy of the interface of a LC is dependent on the orientation of the LC at the interface.[22–24] For a LC sample with a uniform azimuthal orientation at an interface, the orientation-dependent interfacial energy density can be approximated by the Rapini−Papoular expression, $f_s=W_d\sin^2(\theta-\theta_e)$, where θ and θ_e are the actual and equilibrium tilt angles of the LC at the interface, respectively, and W_d is anchoring energy coefficient. The latter quantity is typically $10^{-7} – 10^{-4}$ J/m^2 and thus orders of magnitude smaller than the overall interfacial free energy density ($10^{-3} – 10^{-2}$ J/m^2) of most oil-water interfaces. The small magnitude of the interfacial anchoring

energy of a LC means that subtle interactions at a LC interface (e.g., caused by adsorption of a surfactant) can cause changes in the orientations of LCs. In this context, LCs have been used to report a wide range of molecular/microscopic events at interfaces, such as supramolecular clustering of amphiphiles,[25] photoisomerization,[26,27] enzymatic reactions,[28] formation of DNA complexes,[29] directed assembly of oligopeptides,[30] and interfacial interactions of ions.[31,32] In most past reports, however, the optical responses of LCs to these molecular stimuli have been studied in the absence of flow (see below for additional comments). Here we move to study flow-induced organizations of amphiphiles at LC interfaces.

Finally, while some LCs exhibit a tumbling response to a shear flow, other LCs such as 5CB align along the direction of the shear flow due to orientation-dependent viscosities (characterized by Leslie viscosity coefficients, α_n).[23] Specifically, the shear stress within a film of flowing LC can be approximated as $\tau = dv/dz(\alpha_2 cos^2\theta - \alpha_3 sin^2\theta)$, where v is the velocity parallel to the film interface and α_2 and α_3 are Leslie coefficients. Because the shear stress is orientation-dependent, the LC within a sheared film of 5CB will experience a torque until opposed by a torque generated by elastic stresses.[33] Accordingly, the orientational response of the LC enables visualization of the shearing of the LC.[34] While a number of past studies have reported that LCs sheared between plates undergo shear-alignment,[35,36] more recently it has been observed that microscopic phenomena[37–40] such as the motion of bacteria can lead to shear alignment of LCs.[41] Additionally, the interfacial spreading of phospholipid from single vesicles has been observed to transiently reorient LCs and permit visualization of the interaction of single vesicles with LC interfaces.[25] How flow induces realignment of LCs in the presence of adsorbed amphiphiles, including flow-induced reorganization of amphiphiles, has not been explored in detail. Understanding the coupling of flow and surfactant organization at aqueous interfaces may further

provide fundamental insights into the origins of the spontaneous propulsion of LC droplets in concentrated aqueous surfactant solutions.[42–46]

Our experimental approach to exploring flow-induced reorganization of surfactants at LC-water interfaces is based on use of a millifluidic channel within which 20 micrometer-thick films of nematic 5CB are hosted (Figure 1). We hypothesized that reorganization of amphiphiles at LC-aqueous interfaces in the presence of flow would be optically reported by the LC through a range of phenomena, including the influence of local surfactant concentrations on the LC anchoring

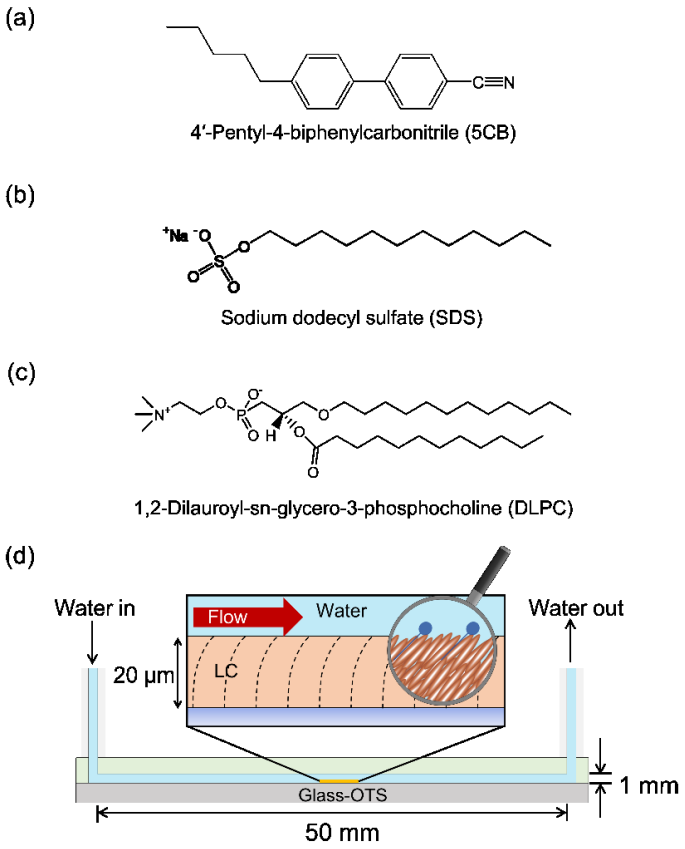

Figure 1. Molecular structures of (a) 5CB, (b) SDS and (c) DLPC (d) Schematic illustration (side view) of the millifluidic channel used to measure the optical response of LC films (thickness of 20 µm) to flowing aqueous surfactant solutions.

energy density (W_d), the effect of local surfactant concentration on the easy axis of the LC (θ_e), and the effects of Marangoni stresses on the mobility of the LC interface and thus the shearing of the LC. Our study aimed to determine which of these factors dominated the orientational behavior of the LC in the presence of a flowing surfactant solution and, more broadly, to explore the utility of nematic LCs as responsive materials for analyzing non-equilibrium states of amphiphiles at water-oil interfaces.

EXPERIMENTAL SECTION

Preparation of octyltrichlorosilane-coated glass slides. Glass microscope slides (Fisher Scientific) were cleaned with Alconox detergent using deionized water and ethanol (Fisher Scientific), and then incubated in Nochromix solution (a mixture of Nochromix and 98 % sulfuric acid) for 1 day. The slides were thoroughly rinsed with 100 ml of deionized water 5 times and then dried under a stream of gaseous N_2. The clean glass slides were then incubated in 1 vol. % octyltrichlorosilane (OTS, Sigma-Aldrich) in hexane (Fisher Scientific) for 30 mins. After silanization, the glass slides were washed sequentially with hexane (100 ml), chloroform (100 ml × 3) and water (100 ml).

Fabrication of millifluidic channels. A schematic illustration of a millifluidic channel is shown in Figure 1d and Figure S1 (in Supporting Information, SI). The millifluidic channels were composed of 3 layers. The top two layers were laser-cut acrylic sheets (thickness of 1 mm from ZLazr.com, USA) and the bottom layer was a glass microscope slide treated with OTS as described above. The laser-cut acrylic sheets were bonded by applying dichloromethane to the contacting surfaces of the sheets. After bonding, the acrylic sheets were cleaned by sequential immersion in glass staining jars filled with 100 ml of water, acetone, ethanol, and hexane. Any residual solvent was removed by evaporation using a gaseous N_2 stream.

The inlet and outlet ports of the millifluidic channel were connected to tubing (Platinum-Cured Silicone Tubing, Fisher Scientific) and sealed with polydimethylsiloxane (PDMS, Sylgard 184, Dow Chemical). The silicone tubing attached to the inlet port was then connected to a syringe (20 ml, Henke-Sass Wolf, Germany) mounted in a multi-channel syringe pump (KD Scientific). The syringe was washed with ethanol and water prior to use.

We placed a metallic TEM grid (pores of 75 mesh) at the center of an OTS-treated glass slide that was positioned on a hot plate (60 °C). The grid was oriented on the glass slide such that the leading edge of each square within the grid was perpendicular to the direction of flow of the aqueous phase in the millifluidic channel. Next, 0.2 μl of 5CB (HCCH, Jiangsu Hecheng Display Technology Co., Ltd.) was injected into the TEM grid. The excess 5CB was removed from the grid using a micropipette tip. The OTS-treated glass substrate supporting the TEM grid was covered by the top acrylic sheet (Figure S1), and the flow cell was held together using bulldog clips. We replaced the air-filled millifluidic channel with aqueous solution using a syringe pump. To establish that the interface of each LC film was flat, we characterized interference colors (bands) generated by any curvature of the LC interface (if the TEM grid was under filled or over filled) in water by using an optical microscope. We used LC films exhibiting either 1 or 2 distinct interference colors (see Figure 2a for an example) in the experiments reported in this paper.

Preparation of DLPC-decorated LC-water interfaces. We used DLPC (Figure 1c, Avanti, Alabaster, AL, USA) as an insoluble amphiphile to decorate the LC-water interface. Prior to depositing DLPC on the interface, the LC films were sheared with SDS (Figure 1b, Sigma-Aldrich) as a control experiment to validate sample preparation. The aqueous SDS phase was then rinsed with 100 ml of deionized water (from a Milli-Q water purification system) three times and replaced with 25 μM DLPC in aqueous 300 mM NaCl. To prepare the aqueous 25 μM DLPC dispersion

of vesicles, we dried DLPC in chloroform (25 mg/ml) onto the surface of a glass vial using a stream of gaseous nitrogen. The vial was then vortexed with a volume of aqueous 300 mM NaCl that generated a DLPC concentration of 25 μM. The DLPC solution was pumped into the millifluidic channel using the syringe pump, displacing the DI water present in the millifluidic channel. The LC films were incubated against the DLPC solution for 30 mins without shearing. During incubation, the LC films gradually transitioned from a bright optical appearance to a dark optical appearance when observed between crossed polarizers on a microscope.

Microscopy and retardance measurements. An optical microscope (Olympus BX41) equipped with 4×, 10×, and 50× objectives, two rotating polarizers, a Moticam 10.0 MP camera and a halogen lamp (philips 6V 30W bulb) for light illumination was used. To analyze time-dependent changes in the optical retardance of LC films, we compared the interference colors of LC films to a calibration chart. To make the calibration chart, we made a wedge cell filled with 5CB. The wedge cell was assembled from glass plates coated with polyimide (PI 2555), rubbed with velvet cloth to achieve unidirectional alignment of the LC director, and paired in an anti-parallel manner (see SI). The dimensions of each glass plate were 75 mm by 26 mm. The thickness of the LC at one end of the wedge cell was ~ 6 μm and the other end was ~ 500 nm. Optical retardance values of the LC in the wedge cell were measured with a PolScope. Micrographs of the wedge cell were split into red, green, blue color channels with ImageJ. Each color signal was quantified with ImageJ. The optical signal was then plotted against retardance. Additional detail regarding the procedure used to estimate the retardance is given in SI.

RESULTS AND DISCUSSION

The goal of our initial experiment was to characterize the dynamic optical response of a flat LC interface to a flowing aqueous solution of SDS using the experimental set-up shown in Figure 1d. As detailed in the Experimental section, 5CB films were formed within metallic TEM grids (~20 μm in thickness, 284 μm × 284 μm individual grid square size) placed

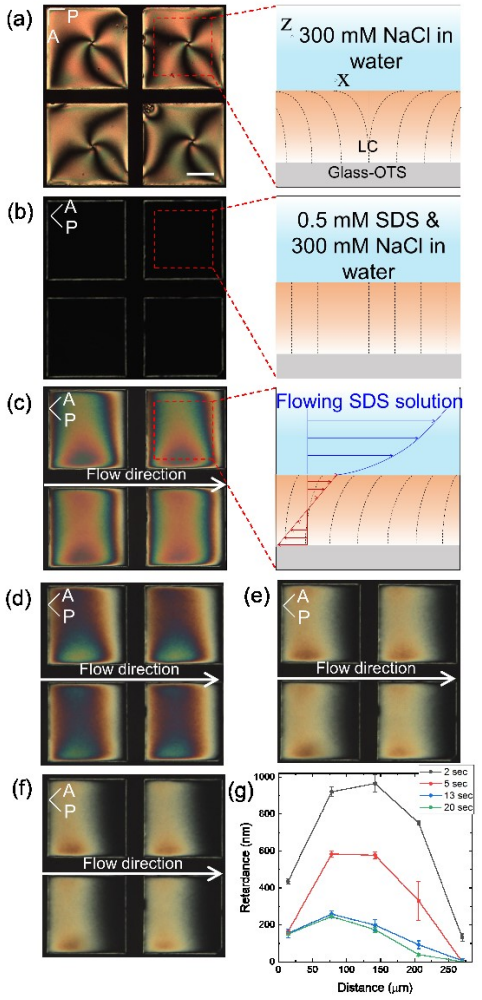

Figure 2. Micrographs (cross-polars) of LC films confined within square TEM grids. The orientations of the analyzer and polarizer are indicated in the top left of each micrograph. The LC films shown are in contact with (a) aqueous 300 mM NaCl (not flowing), (b) aqueous 0.5 mM SDS (not flowing), (c) aqueous 0.5 mM SDS approximately ~ 2 sec after the onset of flow in the millifluidic channel at an area-average velocity of 200 mm/sec, (d) aqueous 0.5 mM SDS approximately ~ 5 sec after onset of the flow, (e) aqueous 0.5 mM SDS approximately ~ 13 sec after the onset of flow, and (f) flowing aqueous 0.5 mM SDS at steady state (20 sec after the onset of flow). (g) Spatial variation in optical retardance measured across the LC films approximately 2 sec and 20 sec after the onset of flow. Error bar: S.D. with n = 4 and scale bar: 100 μm.

on a glass slide treated with octyltrichlorosilane (OTS). The OTS-treated glass supporting the TEM grid was placed into a millifluidic channel (Figure 1d). Next, the millifluidic channel was filled with aqueous NaCl solution using a syringe pump. We added 300 mM NaCl to the aqueous phase to prevent formation of microdroplets of water at the LC-OTS-treated glass interface, as discussed previously.[47] When the LC films were incubated against stagnant 300 mM NaCl aqueous solutions, the films exhibited a Schlieren texture comprising a bright optical appearance (between crossed polars) with dark brushes originating from the center of the LC film within each grid square (Figure 2a). 5CB is known to assume a perpendicular (homeotropic) orientation at the surface of OTS-coated glass, and thus the bright optical texture is consistent with tilted or planar anchoring of the LC at the LC-water interface.[22,25,31] The dark brushes correspond to regions of the LC film in which the azimuthal projection of the LC director is aligned either parallel or perpendicular to one of the crossed polarizers.[48] In contrast, when incubated against stagnant solutions of 0.5 mM SDS in 300 mM NaCl (critical micelle concentration of SDS in 300 mM NaCl is 0.57 mM), the LC films exhibited a uniformly dark optical appearance (Figure 2b), consistent with LC oriented perpendicular to the SDS-decorated LC-water interface.[19,49]

When the LC films in Figure 2b were sheared by initiating flow of the aqueous 0.5 mM SDS solution (in 300 mM NaCl) through the millifluidic channel at an area-average linear velocity of 200 mm/sec, we observed the LC film to exhibit a time-dependent change in optical appearance when viewed between crossed polars oriented at 45° to the flow direction (Figure 2c-f). At this flow rate, as detailed later in this paper, the maximum LC interfacial velocity ($V_{x,int}$) was 14 μm/sec, which corresponds to a capillary number of 1×10^{-4}, where the capillary number is evaluated as $Ca = v_{x,int}\, \eta/\sigma$, and η is viscosity of 5CB (approximated here as 30 mPa.s, which corresponds to an isotropic phase of 5CB[50]) and σ is interfacial tension (4.1 mN/m with the SDS solution, as

measured by the pendent drop method; see Figure S6). The small Ca number (10^{-4}) is consistent with our experimental observation that the shape of the LC interface did not change measurably with onset of the flow.

During the 2 sec period of time that followed the onset of flow of the SDS solution, the LC developed a bright optical appearance (Figure 2c, See Video 1). We quantified the optical retardance of the LC film at t = 2 s by analyzing the interference colors and intensity of light transmitted through the LC (see SI for details). As shown in Figure 2g, the optical retardance, measured as a function of the distance from the upstream edge of the LC film within a grid square, was found to be maximal near the center of the LC interface, with an average value (averaged along the flow direction) of r = 641 ± 15 nm. For reference, the optical retardance of the hybrid configuration of the LC film (e.g., corresponding to the LC at rest in aqueous NaCl) is approximately 1800 nm. These results indicate that the LC film tilted away from the surface normal at the aqueous-LC interface in the presence of the flowing SDS solution, with a tilt angle (from the interface normal) that was substantially less than 90^{o} (see below for additional quantification of the tilt angle).

Inspection of Figure 2c also reveals a spatial variation of the magnitude of the optical retardance across the LC interface in a direction perpendicular to the flow direction (low retardance of the LC near the TEM grid surface). The intensity and the range of interference colors measured in the direction perpendicular to the flow was observed to vary between experiments, and thus reflects sample-to-sample variation in the experimental geometry (See Figure 2c, Figure S4a. and Figure S7a). Below we focus our observations on spatial and temporal changes in the LC optical retardance in the direction of the aqueous flow, features of the system that were found to be reproducible across multiple samples.

Subsequent to the initial bright appearance of the LC film, as described above, we observed the optical retardance of the LC film to decrease continuously with time, with average values of the retardance decreasing from 641 ± 15 nm (2 sec, Figure 2c) to 331 ± 16 nm (5 sec, Figure 2d) and ultimately to 142 ± 14 nm (13 sec, Figure 2e), as shown in Figure 2g. Simultaneously, along with the decrease in average retardance, the local region of the interface exhibiting the highest optical retardance gradually moved from the center of the LC domain towards the upstream side of the LC interface (Figure 2g). At steady state (reached after approximately 13 s), we measured the optical retardance to show a weak maximum on the upstream side of the LC film, with the retardance changing from 150 ± 7 nm near the upstream edge of the LC to less than 12 nm at the downstream edge of the film (Figure 2f). This steady state of the system was maintained for as long as the flow of the SDS solution was sustained, and it was observed across multiple independently prepared samples. Additionally, we repeated the experiments described above with one of the cross-polarizers oriented parallel to the direction of the aqueous flow. In these experiments, we measured no change in optical retardance of the LC with onset of flow, indicating that the flow-induced tilt of the LC occurs in an azimuthal direction that is parallel to the aqueous flow direction (Figure S3).

Our experimental observations also revealed that the LC interface within each grid square of the TEM grid behaved in a manner that was largely decoupled from the adjacent grid squares. In contrast, TEM grids that were overfilled with LC created a single LC interface that spanned multiple grid squares: The LC within an overfilled grid exhibited an optical response that was contiguous across multiple grid squares of the TEM grid and was much brighter (values of retardance of up to 1600 nm) than the optical response of a LC interface that was

compartmentalized within a single grid square (e.g. Figure 2f). In this paper, we do not report results obtained with overfilled TEM grids.

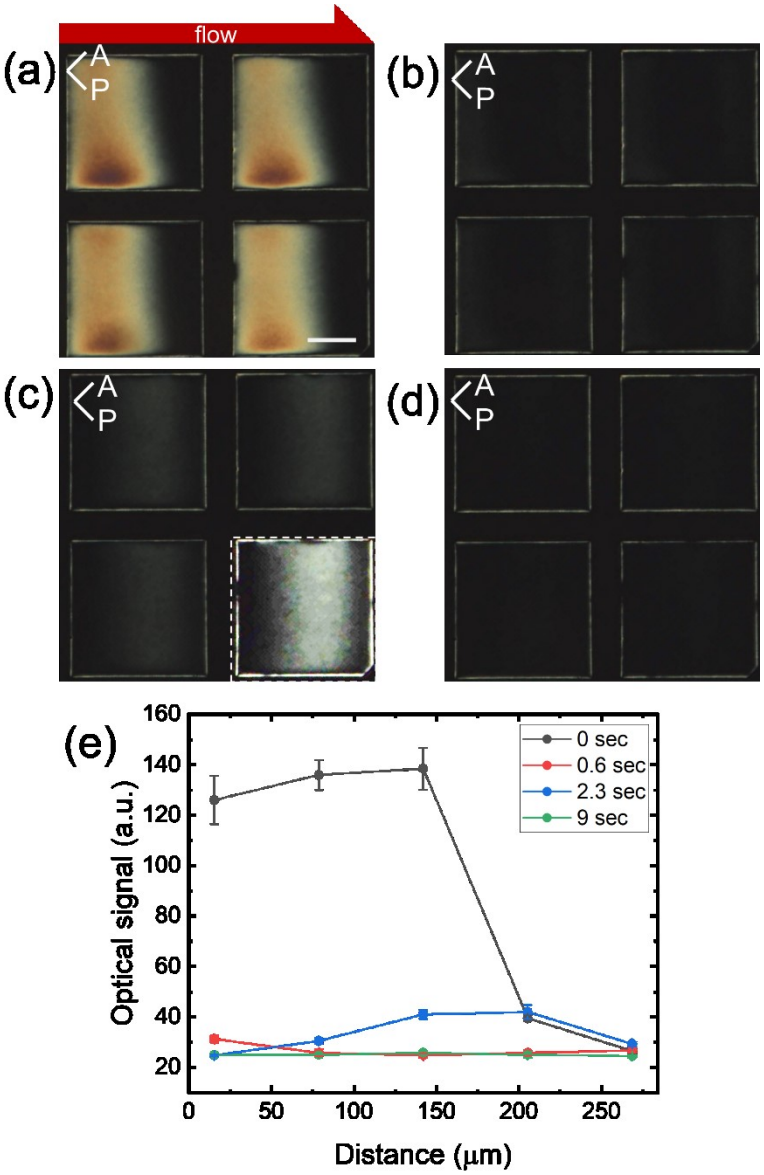

Figure 3. Micrographs (crossed-polars) of LC films after cessation of flow (at area-average velocity of 200 mm/sec in a millifluidic channel) of an aqueous 0.5 mM SDS solution. (a) LC film just prior to stopping the flow. (b) LC film approximately 0.6 sec after stopping the flow. (c) LC film approximately 2.3 sec after stopping the flow. (d) LC film approximately 9 sec after stopping the flow. (Scale bar: 100 μm) Brightness and contrast of one of the TEM grid squares (dotted line) in (c) were adjusted to aid visualization of the optical signal. (e) Position-dependent change in optical signal (intensity of transmitted light) from LC films as a function of time following cessation of flow described in a-d. (error bar: S.D. with n = 4)

After characterizing the steady state shown in Figure 2f, we stopped pumping the SDS solution through the millifluidic channel. Within 0.6 sec of cessation of pumping, the steady state optical texture (Figure 3a) evolved to a transient state that exhibited negligible optical retardance (Figure 3b). Subsequently, after an additional ~ 2 s, a bright band (Figure 3c, optical contrast and brightness in lower right grid square has been enhanced for visualization) was observed to move from the downstream side of the LC film to the upstream side within each grid square. The transit

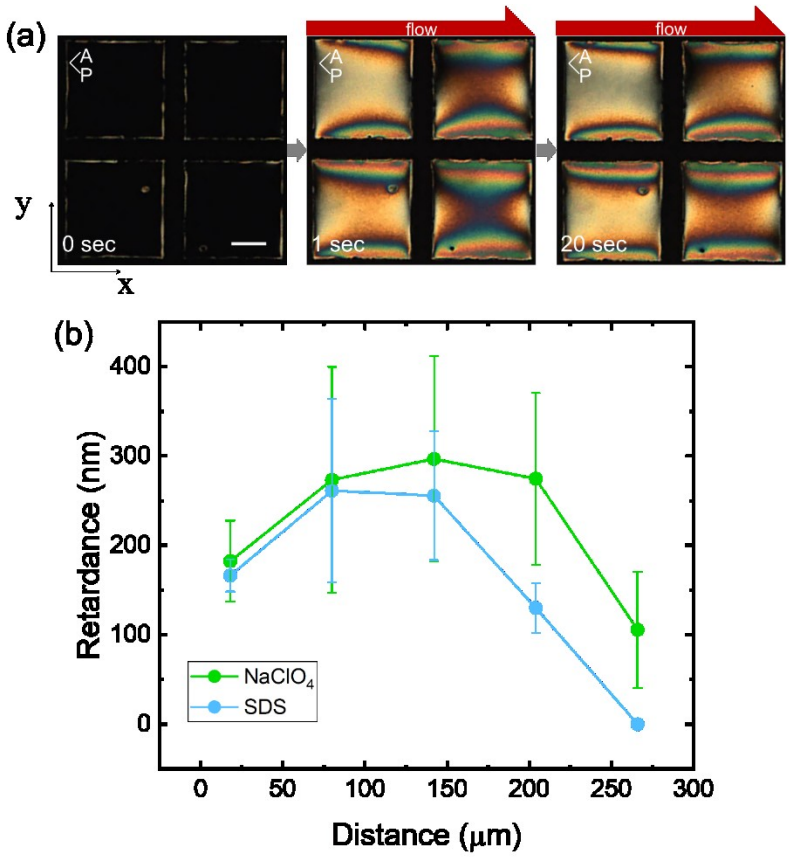

Figure 4. Comparison of the optical response of LC films to aqueous solutions of 2 M sodium perchlorate and 0.5 mM SDS in 300 mM NaCl. (a) Optical micrographs (cross-polars) of LC films incubated in 2 M $NaClO_4$ in the absence of flow (left), LC films in contact with flowing $NaClO_4$ solution for 1 sec (middle) and 20 sec (right) at an area-average velocity of 200 mm/sec in a millifluidic channel (scale bar: 100 μm). (b) Steady state optical retardance of LC films in contact with the flowing aqueous solutions of SDS and $NaClO_4$ as a function of distance from the leading edge of each LC film (error bar: S.D. with n = 3).

of the bright band across the LC film took ~ 6 sec, and ended with the LC film resuming a uniformly dark state (Figure 3d,e). The final dark state corresponded to a homeotropically oriented film.

We hypothesized that the spatial and temporal optical responses of the LC films, as presented in Figures 2 and 3, likely reflected both the motion of the LC interface and reorganization of SDS molecules on the LC interface. To provide further insight into the role of the SDS, we performed an experiment under the same flow conditions but without SDS in the aqueous phase. To achieve a perpendicular orientation of LC at the aqueous interface without SDS, guided by our prior studies, we added 2 M sodium perchlorate ($NaClO_4$) to the aqueous phase (Figure 4a).[31] When the aqueous sodium perchlorate solution was flowed past the LC interface at a linear area-average velocity of 200 mm/sec, we observed the LC film to assume a bright optical appearance with an average retardance of 267 ± 97 nm within ~ 1 sec. In contrast to our observations with flowing SDS solutions (Figures 2 and 3), however, the uniform bright optical appearance of the LC was not a transient state but was sustained for the duration of the flow (Figure 4b). Additionally, the LC exhibited a spatial variation in retardance that was maximal at the center of the LC film (Figure 4b). This contrasts also to our observations when using the flowing aqueous SDS solution, where the maximum in retardance was displaced towards the upstream side of the LC interface (Figure 4b). As a control experiment, we displaced the sodium perchlorate solution by aqueous 300 mM NaCl, and then flowed 0.5 mM SDS (in aqueous 300 mM NaCl) at 200 mm/sec. We confirmed that an optical response of the type shown in Figure 2 was observed (see also Figure S4a). Overall, the striking difference in dynamic and steady state response that we observed when flowing aqueous SDS versus sodium perchlorate, including differences in the retardance measured on the downstream side of the LC film at steady state (106 ± 65 nm and < 12

nm for sodium perchlorate and SDS, respectively), led us to conclude that the optical response of the LC observed with flowing aqueous SDS is influenced by the lateral organization of the SDS on the LC interface (Figure S4b,c).

We also interpret the spatial variation in the optical retardance of the LC film in contact with aqueous perchlorate solution (decrease at upstream and downstream edges of the LC film), as shown in Figure 4b, to reflect the presence of a circulating flow of LC that is internal to the LC film (Figure S2).[51,52] We measured the tangential velocity of the LC-aqueous interface associated with this flow to decrease near the edges of the grid, as compared to that at the center of the grid. Because 5CB is a flow aligning LC,[22] the tilt of the LC away from the surface normal is, therefore, smaller near the edges of the LC domain (lower optical retardance of the LC film). As discussed below, we conclude that the SDS on the interface of the LC substantially changes the mobility (velocity) of the LC as compared to the perchlorate solution, and thus alters the flow internal to the LC (relative to perchlorate solution) and optical response of the LC.

Past studies have demonstrated that amphiphiles can be advected along fluid interfaces in the flow direction, leading to lower concentrations (relative to the downstream side) on the upstream side of the interface and elevated concentrations (relative to the equilibrium concentration) on the downstream side of the interface.[1,9] The resulting spatial gradient in interfacial concentration of the amphiphiles generates a Marangoni stress, which in turn opposes the shear stress exerted by the flowing aqueous phase and thus decreases the mobility of the interface.[1,12,21] The magnitude of the interfacial concentration gradient of amphiphiles is influenced by the rate of adsorption of the amphiphiles on the upstream side of the interface and the rate of desorption on the downstream side. Past studies of ionic surfactants such as SDS at high ionic strengths have established that the kinetic barriers to adsorption are small and that the flux

of surfactant onto the interface is typically diffusion-controlled. [15,53] In the discussion below, we assume that SDS adsorption onto the upstream side of the LC interface is diffusion-controlled. The flux of SDS leaving the LC interface on the downstream side will be controlled by the kinetics of desorption of SDS from the LC interface. These considerations led us to explore two limiting interpretations of the dynamic and steady state optical responses of the LC reported in Figure 2 (Figure S4a). We summarize our proposals in Figure 5. Our first proposal is that the position-dependent variation of the LC optical retardance at steady state in Figure 2f is influenced by the presence of SDS because the SDS is advected towards the downstream side of the LC interface, thus depleting the upstream side of the LC interface of an interfacial surfactant concentration that is sufficient to sustain perpendicular anchoring of the LC (Figure 5a-c). That is, our first proposal interprets the effect of SDS on the variation in orientation of the LC to be dominated by variation in the interfacial surfactant concentration, resulting in a change in the easy axis (lowest free energy orientation; θ_e) of the LC at the aqueous interface. As depicted in Figure 2c, when analyzing this limiting behavior, we neglect the effect of the mobility of the interface (and thus shearing of the LC) on the orientational response of the LC (the effects of interfacial mobility are explored below).

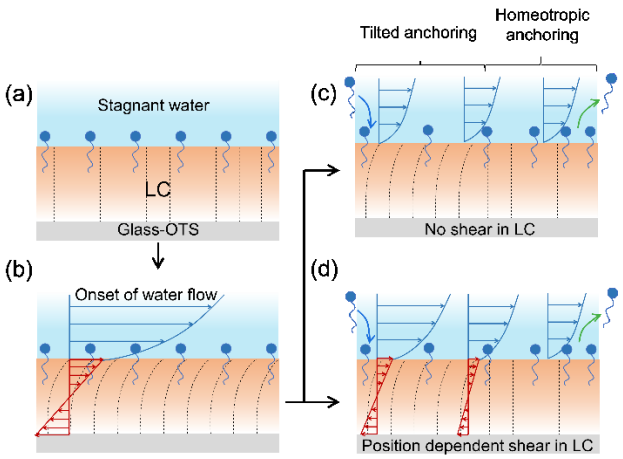

Figure 5. Schematic illustrations conveying possible mechanisms leading to the optical responses of LC films to flowing aqueous surfactant solutions: (a) Equilibrium orientation of LC in the absence of flow of a surfactant solution; the LC is shown to align perpendicular to the interface

with a uniform concentration of SDS across the interface, (b) Schematic illustration of transient state of the LC interface immediately after the onset of flow of the aqueous surfactant solution; the interface of the LC is mobile, resulting in shearing and reorientation of the LC. (c) Schematic illustration of steady state response of LC in the presence of flowing surfactant solution; as shown, the surfactant concentration gradient across the LC interface generates a change in the orientation of the easy axis of the LC. The interface is assumed to be effectively immobile, and thus the LC does not reorient due to shear. (d) Schematic illustration of steady state response of LC in the presence of flowing surfactant solution; as shown, the surfactant concentration gradient across the LC interface generates a Marangoni stress that is largest on the downstream side of the LC interface. In the scenario depicted in d, the Marangoni stress regulates the mobility of the interface and thus the rate of shearing of the LC (and thus the extent to which the LC reorients across the LC film).

To explore our first proposed mechanism, we estimated the Marangoni stress that would arise from a gradient in surfactant concentration sufficiently large to cause the LC to change from a homeotropic to tilted orientation. The interfacial concentration of surfactant on the downstream side of the LC interface was estimated as that present in the absence of flow of aqueous 0.5 mM SDS (in 300 mM NaCl). This estimate is a lower bound on the actual value, as discussed above. By using a pendant drop to measure interfacial tension, we determined the surface pressure of the SDS at the stationary LC-aqueous interface to be 23 ± 0.2 mN/m (see Figure S5 and Figure S6). In contrast, at equilibrium, we determined the maximum concentration of SDS in 300 mM NaCl that sustains a tilt of the LC away from the normal to be 0.016 mM with a corresponding surface pressure of 5.6 ± 0.5 mN/m. Thus, if the optical response of the LC reflects a flow-induced decrease in interfacial concentration of SDS at the upstream side of the LC interface (and thus change in the orientation of the easy axis of the LC), the change in surface pressure across the LC interface would be greater than ~ 17.4 mN/m (the arguments described above provide a lower bound on the magnitude). This change in surface pressure corresponds to a Marangoni stress of $\tau_{Ma} = \Delta\gamma/\Delta x = 61$ Pa, where Δx (284 μm) is the width of TEM grid square used in our experiment. In contrast, we estimate the upper bound on the shear stress exerted on the LC-water interface as $\tau_{water} = 6\eta Q/h^2W = 1.07$ Pa, where η, Q, h and W are the viscosity of water (8.9×10^{-4} Pa.s),

volumetric flow rate (1 ml/sec), height of the channel (1 mm) and width of the channel (5 mm).[9] This estimate assumes that the interface of the LC is immobile, and thus the actual interfacial shear stress due to the flow of the aqueous phase will be less than 1.07 Pa. The key conclusion of this analysis is that the Marangoni stress predicted by our first proposal (61 Pa) is an order of magnitude larger than the interfacial shear stress (1.07 Pa) imposed by the flow of the aqueous SDS. As the magnitude of the Marangoni stress is bounded by the wall shear stress generated by the flow, we conclude that a spatial gradient in surfactant concentration alone cannot account for the optical response of the LC shown in Figure 2f.

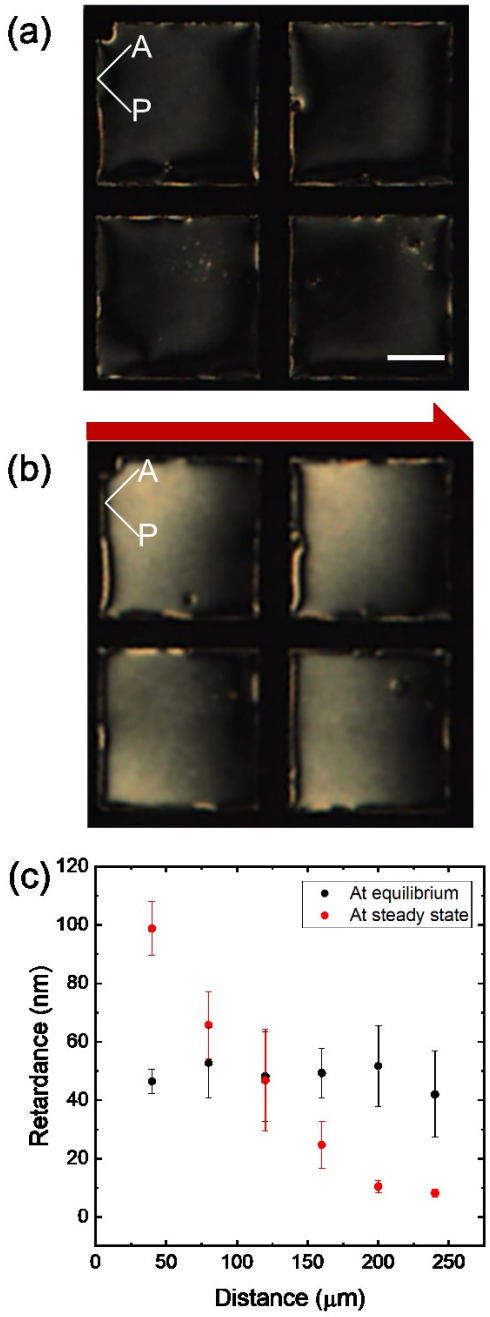

Figure 6. (a-b) Optical micrographs (crossed polars) of 5CB films in contact with aqueous solutions of 0.015 mM SDS (a) in the absence of flow, (b) flowing at an area-average velocity of 200 mm/sec (at steady state). (Scale bar: 100 μm) (c) Equilibrium (no flow) and steady state retardance of LC films in contact with aqueous solutions of 0.015 mM SDS as a function of distance from the leading edge of each LC film (error bar: S.D. with n = 4).

Although the argument above leads us to conclude that gradients in interfacial SDS concentration alone (via a change in the orientation of the easy axis of the LC) cannot provide an account for the spatial gradient in orientation of the LC induced by the flowing SDS solution, additional experimental evidence does support our conclusion that spatial gradients in surfactant concentration are present on the LC interface. Specifically, we performed experiments with aqueous solutions of 0.015 mM SDS (in 300 mM NaCl), which caused LC films at equilibrium (no flow) to exhibit weak birefringence (retardance = 48 ± 4 nm). This value of retardance corresponds to a surface tilt angle of the LC director of 12.5 ± 0.5° from the normal of the aqueous-LC interface (Figure 6a). Following the onset of flow, similar to the experiments reported in Figure 2 and 3, we observed a transient increase in brightness of the LC film, followed by the appearance of a steady state that was characterized a spatial gradient in optical retardance across the LC film (Figure 6b). In contrast to the result obtained with flowing 0.5 mM SDS, however, we observed flowing 0.015 mM SDS solution to cause the optical retardance of the LC on the downstream side of the LC film to decrease relative to that measured in the absence of flow (8 ± 1 nm vs. 48 ± 4 nm, respectively; Figure 6c). The decrease in optical retardance of the LC film induced by the fluid flow indicates that the interfacial concentration of SDS near the downstream side of the LC must be higher than that of the same region of the interface at equilibrium. From the optical response of the LC in this experiment, we conclude that SDS molecules on the LC interface are advected to the downstream side of the LC film leading to an increase in the interfacial concentration. Thus, while spatial gradients in interfacial surfactant concentration are not sufficient alone to cause the gradients in LC orientation that we observe at steady state in the presence of flowing 0.5 mM SDS, the experiment above performed with 0.015 mM SDS demonstrates that gradients in interfacial SDS concentration are present on the LC interface.

The results above led us to propose a second mechanism (limiting behavior) by which the spatial and temporal response of the LC to the flowing 0.5 mM SDS solution is generated (Figure 5d). We hypothesized that the influence of SDS on the optical appearance of the LC film at steady state (Figure 2f) reflects spatial variation in the mobility of the LC interface due to Marangoni stresses generated by advection of SDS across

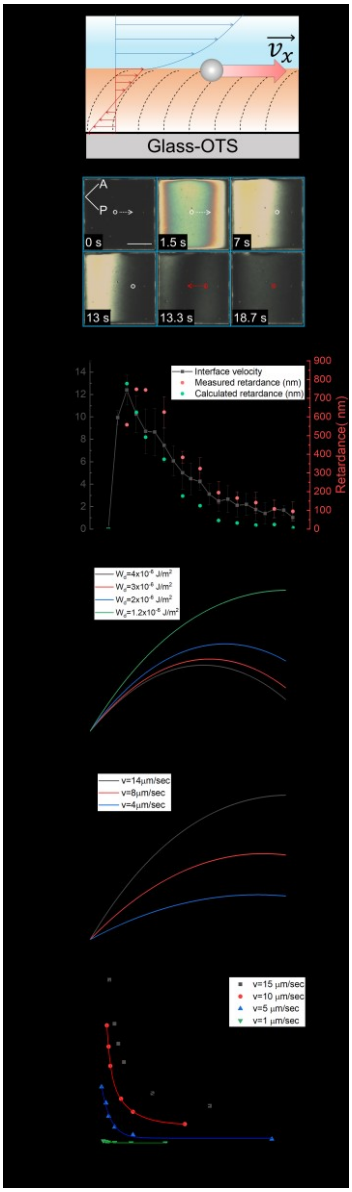

Figure 7. (a) Schematic illustration of a latex particle on a LC-aqueous interface in the presence of a flowing aqueous phase. (b) Time-lapse images showing a change in position of the latex particle with time. The white and red circles and arrows in the images were inserted to indicate the

locations of the latex particle and direction of movement. The white circles and red circles indicate particle location under flow (blue) and after cessation of the flow (red), respectively. (c) Interfacial velocity (dark square dots) and optical retardance (red and green filled circles) plotted as a function of time (at the location of the latex particle). Red circles indicate retardance measured experimentally and green circles indicate retardance calculated from the model described in the text. Error bar: S.D. with n = 3 and scale bar: 100 μm. (d) Calculated LC tilt angle profiles along the z axis of a LC film as a function of the anchoring energy coefficients of the aqueous-LC interface at a fixed $v_{x,int}$ = 13.5 μm/sec. (e) Tilt angle profiles calculated along the z axis of a LC film as a function of $v_{x,int}$ at fixed $W_d = 1.2 \times 10^{-6}$ J/m^2. (f) Retardance of a LC film calculated as a function of W_d and $v_{x,int}$.

the interface. To provide support for this proposal, we measured the mobility (interfacial velocity) of the LC interface by tracking the motion of latex particles adsorbed at the LC-water interface (Figure 7a and b). We adsorbed particles onto the LC-aqueous interface at rest, and then initiated pumping of aqueous SDS solutions at an area-average linear velocity of 200 mm/sec past the LC interface. Inspection of Figure 7c reveals that a tracer particle initially located near the center of the LC interface (to minimize flow effects associated with the edge of the grid square; the particle was located 99 ± 17 μm from the upstream edge of the LC) was displaced downstream by 52 ± 28 μm over a duration of 10 sec. Following the onset of flow of the aqueous phase, during this displacement, we measured the interfacial velocity to increase to 12 μm/sec and then slow to approximately 1 μm/sec. This qualitative result provides initial support for our proposal that spatial variation in the LC optical response may reflect changes in the mobility of the LC interface due to gradients in interfacial surfactant concentration. We also measured the optical retardance of the LC film at each point on the interface at which we determined the interfacial velocity of the particle. Inspection of Figure 7c reveals that the interfacial velocity is proportional to the optical retardance. We return to this observation below.

To evaluate further our second proposed mechanism, we constructed a simple mechanical model of the LC film. The model contains a number of approximations. In particular, we assume

that the LC response shown at each time point in Figure 7b can be approximated as a local steady state. This assumption is justified by a prior analysis indicating that, following imposition of a given surface velocity, steady-state velocity and orientational profiles across the LC film will be established within 1 μs.[25] Additionally, as noted in the Introduction, within the LC film, we describe the orientation of the LC as arising from a balance between torques due to elastic strain of the LC film and the anisotropic viscosities of the LC (see SI for a more complete analysis),[22,54] leading to the equation

$$K\frac{\partial^2\theta}{\partial z^2} = \frac{v_{x,\,int}}{d}(\alpha_2\, cos^2\,\theta - \alpha_3\, sin^2\,\theta) \quad (1)$$

where K ~ 10^{-11} N is the elastic constant of the LC (using one parameter approximation) and α_3 ~ -2 × 10^{-3} kg/ms and α_2 ~ -83 × 10^{-3} kg/ms are the Leslie viscosity coefficients of 5CB,[23] $v_{x,int}$ is the LC-water interfacial velocity, z is position in LC film in the vertical direction, and θ is the tilt angle of the LC from the film normal. Many past studies of LC hydrodynamics at solid surfaces have assumed strong anchoring of LCs,[23,33,55] such that the LC orientation at the interface is shear rate-independent. Aqueous interfaces, however, typically lead to weak anchoring of LCs and thus we assume that the LC tilt angle is dependent on both the anchoring energy coefficient, W_d, and surface shear stress. To determine the tilt angle of the LC at the LC-water interface, we used a torque balance, namely

$$\left|\left[K\left(\frac{\partial\theta}{\partial z}\right)\right]_{z=d}\right| + |[W_d\, sin(\theta)\, cos(\theta)]_{z=d}| = |\tau z|_{z=d}| \quad (2)$$

where τ is approximated as (α_2 $\cos^2\theta_d$ – α_3 $\sin^2\theta_d$) $v_{x,int}$/d and θ_d is the LC tilt angle at the aqueous-LC interface (z = d). By solving eqn (1) and (2) simultaneously, we calculated LC tilt angle profiles across the LC film as a function of W_d and $v_{x,int}$ (see Figure 7d–f). For each of the calculated tilt angle profiles, we also evaluated the corresponding value of the optical retardance as

$$\Delta r = \int_0^d \left(\frac{n_e n_o}{\sqrt{n_o^2 \sin^2\theta + n_e^2 \cos^2\theta}} - n_o \right) dz \quad (3)$$

where n_e and n_o are the extraordinary (1.71) and ordinary refractive (1.53) index of 5CB, respectively. By using experimentally measured velocities and eqns (1-3), we determined the value of W_d that provided the closest agreement between measured (Figure 7c) and calculated (eqn (3)) values of optical retardance (see below for an analysis that permits W_d to vary across the interface). The good agreement between experiment and model evident in Figure 7c when using W_d=1.17×10^{-6} J/m^2 suggests that the optical response of the LC to flowing aqueous 0.5 mM SDS (measured along the tracer particle trajectory in Figure 7b) arises largely from the influence of the interfacial surfactant concentration gradient (Marangoni stress) on the mobility of the interface (shear-induced reorientation). The measured spatial gradient in optical appearance of the LC at steady state also indicates that the Marangoni stress is larger near the downstream side of the LC film as compared to the upstream region (i.e., the interfacial mobility on the downstream side of LC is lower than the upstream side).

Additional support for the above conclusion comes from our observations of the relaxation of the LC optical appearance after cessation of the aqueous SDS flow (Figure 7b). As noted above, during the relaxation process, we observed a transient state of the LC involving a bright optical band that past across the sample over ~ 7 sec (see Figure 3 and accompanying text). During the transient optical state, we also observed adsorbed latex tracer particles to translate across the interface in the upstream direction. This backflow at the interface is consistent with the presence of a spatial gradient in interfacial surfactant concentration driving the flow. The SDS that is non-uniformly distributed across the LC interface by the flowing SDS solution is redistributing itself to achieve a uniform coverage, thus generating bright shear bands in the LC film.[1]

The analysis described above employed a spatially invariant value of W_d across the LC interface. However, the inhomogeneous distribution of SDS in the presence of the flowing 0.5 mM SDS leads to the possibility that W_d may vary in magnitude across the interface to impact the LC optical response.[56] To estimate the magnitude of the gradient in surface concentration of SDS and thus W_d, we assumed that the Marangoni stress is balanced by the interfacial shear stress imposed on the LC by the flowing aqueous solution (estimated above as 1.07 Pa). This simple model (see SI for detail) led us to conclude that the change in interfacial concentration of SDS across the LC interface is $\sim 1 \times 10^{-8}$ mol/m^2. A number of past studies have reported the dependence of the LC anchoring energy on surfactant surface concentration,[56] and those past studies lead us to predict that the above-described change in surfactant concentration across the LC interface will cause a change in anchoring energy of $\Delta W_d \sim 0.1 \times 10^{-6}$ J/m^2. This change is an order of magnitude smaller than the anchoring energy coefficient (1.17×10^{-6} J/m^2) that we found to predict the experimentally measured retardance (Figure 7c). We also evaluated how the change in W_d and $v_{x,int}$ would influence retardance, as shown in Figure 7d. For values of the interfacial velocity between 1 and 15 μm/sec, inspection of Figure 7f reveals that retardance decreases with increase in W_d. However, with $\Delta\Gamma \sim 0.01 \times 10^{-6}$ mol/m^2, the impact on the retardance calculated is less than 50 nm or 3 nm for $v_{x,int}$ values of 15 μm/sec and 1 μm/sec, respectively. These changes are small compared to the experimental values of retardance reported in Figure 7c (750 nm at $v_{x,int} \sim 10$ μm/sec and 150 nm at $v_{x,int} \sim 2$ μm/sec). Overall, this analysis leads us to conclude that the variation in the surface anchoring energy (W_d) caused by flow-induced accumulation of surfactant on the LC interface is small for flowing 0.5 mM SDS solution.

The results above, when combined, lead us to the following physical picture, as summarized in Figure 5a, 5b and 5d, regarding how aqueous 0.5 mM SDS impacts the orientation of nematic 5CB in the absence and presence of flow, respectively. In the absence of flow, the LC adopts a homeotropic orientation, consistent with a uniform interfacial concentration of adsorbed SDS (Figure 5a). Upon initiation of flow of the aqueous phase, the LC tilts away from the surface normal, in a direction parallel to the direction of the flow of the aqueous SDS solution. At the onset of the flow, the SDS is homogeneously distributed across the LC interface and thus the Marangoni stress is negligible. Under these conditions, the LC interface is mobile and displacement of the LC-aqueous interface leads to shearing and reorientation (tilting) of the LC. The shearing of the LC film generates to a large and transient optical retardance immediately following the onset of flow of the aqueous phase (Figure 5b). However, with continued flow of the aqueous SDS solution, the SDS adsorbed at the interface is advected downstream, leading to establishment of a gradient in interfacial concentration of SDS, and thus a Marangoni stress that opposes the shear stress imposed on the LC interface by the flowing aqueous SDS. As the Marangoni stress grows in strength at the interface, the mobility of the interface decreases, lowering the shear rate of the LC and thus leading to a decrease in optical retardance of the LC (Figure 5d).

At steady state, in the presence of the flowing aqueous 0.5 mM SDS, we observed the optical retardance/tilt angle of the LC to decrease across the LC film in the direction of the flowing aqueous phase (Figure 7c). We interpret this spatial gradient in optical appearance of the LC to indicate that the Marangoni stress is larger near the downstream side of the LC films as compared to the upstream region. The larger Marangoni stress on the downstream side of the LC leads to a loss of interfacial mobility and thus shearing of the LC. This conclusion is consistent with the

trajectories of tracer particles that we tracked on the LC interface (Figure 7). The high interfacial concentration of SDS near the downstream side of the LC interface also increases the strength of the anchoring energy, thus potentially suppressing the tilt of the LC. For 0.5 mM SDS solutions, however, our estimates of the magnitude of change in anchoring energy across the LC film suggest that the latter effect is not significant in our experiments. Similarly, the gradient in concentration of the SDS along the interface has no measurable effect on the orientation of the easy axis when using 0.5 mM SDS solution.

The magnitude of the Marangoni stress generated by the flowing aqueous SDS solution, as discussed above, is expected to be influenced by the rate of adsorption and desorption of the SDS from the LC-aqueous interface. To explore the response of the LC in the absence of adsorption/desorption, and thus provide additional support for our conclusions regarding the factors controlling the response of the LC to flowing SDS solutions, we performed an experiment using the insoluble amphiphile DLPC at near-saturation coverage (see SI for details). In contrast to SDS, the LC did not exhibit measurable optical retardance following the onset of flow of an aqueous phase of DLPC above the DLPC-decorated LC interface (the orientation of the LC prior to flow was homeotropic). Additionally, when flowing a DLPC-free aqueous phase (300 mM NaCl) across a DLPC-decorated LC interface, there was also no change in the optical retardance of the LC interface (implying negligible desorption of DLPC). Whereas SDS possesses a desorption rate constant of the order of ~0.02 s^{-1} <ref 57>, DLPC does not desorb on the time scale of our experiment.[12,25,53,58]

We interpret our result with DLPC to indicate that, in the absence of desorption of the DLPC from the interface, a Marangoni stress builds rapidly along at the LC interface and thus renders the interface effectively immobile. In addition, other factors such as the surface viscosity

of the DLPC-laden interface likely differ from the SDS-laden interface and thus may also impact the mobility of the interface.[12] More broadly, since Marangoni stresses and interfacial mobility depend strongly on interfacial mass transport and adsorption/desorption kinetics, our result hints that the dynamic optical response of LCs, as described in our study, may offer the basis of new methods for rapidly quantifying the adsorption and desorption kinetics of amphiphiles at oil-water interfaces. We note also that the result described above with DLPC were obtained at near-saturation coverages of the phospholipid (see SI for details). At lower surface coverages, we predict that flow-induced reorganization of the DLPC on the LC interface will likely lead to an optical response of the LC.

Our experimental results obtained using 0.5 mM SDS indicate that the dominant factor that controls the optical response of the LC is the mobility of the interface (as determined by the lateral reorganization of surfactant and Marangoni stress on the interface). This conclusion, however, is specific to this particular concentration of SDS. At lower concentrations of SDS, our results reveal that other physical phenomena at the LC interface measurably influence the optical response of the LC. For example, by using a surfactant at a concentration immediately below that which induces a homeotropic orientation of LC (0.015 mM SDS in 300 mM NaCl), we show that flow-induced reorganization of surfactant can lead to a change in the easy axis of the LC at the LC-water interface (see Figure 6). We conclude, therefore, that with decreasing surfactant concentration, the effect of surfactant on the optical response of the LC changes from (i) being dominated by changes in mobility of the interface due Marangoni stresses generated by surfactant concentration gradients (0.5 mM SDS) to (ii) being dominated by a change in orientation of the easy axis of the LC at the aqueous interface due to interfacial surfactant concentration gradients (0.015 mM SDS).

Our experiments also revealed that the transient optical response of the LC to the onset of flow of the 0.5 mM SDS solution (Figure 2g) differed from that observed with the sodium perchlorate solution. In particular, the maximum optical retardance observed with the SDS solution was >900 nm (measured 2 seconds after the onset of flow), whereas the maximum optical retardance measured using the perchlorate solution was 300 nm (measured immediately after onset of flow and sustained at steady state). This difference is intriguing because, prior to the establishment of Marangoni stresses at these interfaces, the mobilities of the two interfaces are expected to be similar. We speculate that the lower retardance measured when using sodium perchlorate solution (in comparison to 0.5 mM SDS) reflects a higher anchoring energy of 5CB with perchlorate. Support for this proposition can be obtained from Figure 7f, where it is calculated that a change in anchoring energy from 1×10^{-6} J/m^2 to 8×10^{-6} J/m^2 (with a surface velocity of 15 μm/sec) can lead to a change in retardance of the LC from 1000 nm to 200 nm. It is also possible, however, that the interfacial viscosities of 5CB in contact with the SDS and perchlorate solutions may differ from each other.

We conclude our discussion by briefly addressing the relevancy of conclusions based on flowing LC−aqueous interfaces to flowing isotropic oil-water interfaces (both in the presence of surfactants). As discussed above, LCs differ from isotropic oils in a number of important ways, including the presence of orientation-dependent surface energies. We conclude, however, that changes in surface pressure due to surfactant concentration gradients are much larger than surface energy gradients due to changes in the orientation of a LC at an interface. For example, the change in surface pressure across the LC interface in our experiments performed with 0.5 mM SDS can be estimated as $\Delta\Pi = F_{Marangoni}(1.07\ Pa) \times \Delta x\ (\sim 284\ \mu m) = 3 \times 10^{-4}$ N/m while the maximum change in surface energy due to a change in orientation of the LC typically ranges from 10^{-7} to 10^{-}

^{5} N/m. Thus, the orientation-dependent part of the interfacial energy of a LC is small compared to changes in surface energies associated with surfactant-induced Marangoni stresses. While the above analysis suggests that conclusions extracted from studies of surfactant solution flows on LC interfaces are likely relevant to isotropic oils, we note also that an interplay between the elasticity and anchoring of LCs at LC-water interfaces decorated with amphiphiles can trigger the lateral phase separation of amphiphiles into amphiphile-rich phases and amphiphile-lean surface phases.[20,59,60] However, observations of the phase separation of amphiphiles induced by LC elasticity are limited to a narrow range of experimental conditions.[20,59] We did not observe evidence of phase separations during the experiments reported in this paper.

CONCLUSIONS

In summary, this paper describes how the spatial and temporal optical responses of LC oils at LC-aqueous interfaces can be used to report interfacial phenomena associated with flowing aqueous solutions of amphiphiles. Specifically, we show that LCs can be used to report transient interfacial states during the time-dependent evolution of the distributions of surfactant across LC oil-water interfaces following the onset of flow, including facile identification of the time-scale on which the steady state of the interface is established. At steady state, depending on the surfactant concentration, the LC can be used to map spatial variation in the mobility of the LC-aqueous interface, which reflects the presence of Marangoni stresses, or map spatial variation in the surfactant concentration via its influence on the orientation of the easy axis of the LC. Overall, we interpret our experiments to indicate that the dynamic response of the LC is controlled by mass transport of the surfactant from bulk solution onto the LC interface (the kinetics of adsorption of SDS are not rate-limiting at the high ionic strengths used in our experiments), convection of

surfactant along the interface, and the kinetics of desorption of SDS from the interface. We also show that the LC can be used to monitor the relaxation of the surfactant-distribution across the interface following the cessation of the imposed flow. These conclusions are supported by a simple mechanical model of the LC interface, and control experiments performed using salts and insoluble amphiphiles. Overall, our results provide a first step toward understanding how surfactants regulate the response of LCs to flow at LC-aqueous interfaces, including the effects of surfactant reorganization on interfacial mobility (shear of the LC), anchoring energies of the LC, and changes in the easy axis of the LC.

Our results also identify a number of directions for future investigations. First, our study focuses on a select set of surfactant concentrations and a single flow rate. Additional studies are needed to fully understand how surfactant concentration impacts the interplay of interfacial mobility, anchoring energy, and easy axis orientation at LC interfaces in contact with flowing surfactant solutions.[1] Additionally, the role of electrolyte concentration on the optical responses of LCs to flowing surfactant solutions should be investigated as the kinetics of adsorption and desorption of ionic surfactants depend on ionic strength. Second, we interpret the optical responses of the LCs reported in our study to indicate that the downstream interfacial tension gradient is higher than the upstream gradient at steady state when using 0.5 mM SDS. The development of a model for mass and momentum transport, which includes the kinetics of adsorption and desorption of surfactants, would allow us to make a more detailed interpretation of the LC-optical response, Marangoni stresses, and LC shear rates. Third, our study focuses on SDS, and additional studies are needed to understand how surfactant structure impacts the dynamic LC response under flow (including amphiphiles that induce planar anchoring).[61] In particular, previous studies of a large number of surfactants at LC-water interfaces have reported homeotropic anchoring of LCs. We

predict, however, that the non-equilibrium responses of these various surfactants will differ under shear.[19,62] Finally, the approach reported in this paper using LCs can also be potentially extended to multivalent ions or polyelectrolytes that complex with ionic surfactants, where complex dynamics and long-lived non-equilibrium states are often encountered.[17,21]

ASSOCIATED CONTENT

Supporting Information

The Supporting Information is available free of charge at ~~~.

Schematic illustration of a millifluidic channel (Figure S1), schematic illustration of side view of LC confined in a TEM grid (Figure S2), micrographs of LC films under shear (Figure S3), additional results comparing LC response to SDS and $NaClO_4$ (Figure S4), micrographs of LC films in contact with aqueous SDS solutions (Figure S5), interfacial tension of 5CB in SDS aqueous solutions (Figure S6), optical response of LC to aqueous DLPC and SDS (Figure S7), and calibration chart for determining optical retardance (Figure S8). (PDF)

Movie (Video 1) of LC optical response to flowing aqueous 0.5 mM SDS (MP4)

AUTHOR INFORMATION

Corresponding Author

Nicholas L. Abbott − Smith School of Chemical and Biomolecular Engineering, Cornell University, Ithaca, NY 14853, USA; Email: nla34@cornell.edu

Authors

Sangchul Roh − Smith School of Chemical and Biomolecular Engineering, Cornell University, Ithaca, NY 14853, USA

Michael Tsuei − Smith School of Chemical and Biomolecular Engineering, Cornell University, Ithaca, NY 14853, USA

Author Contributions

SR, MT and NLA wrote the manuscript. SR performed the experiments reported in this manuscript. SR, MT and NLA developed the model. SR and NLA analyzed data in the manuscript.

Notes

The authors declare no completing financial interest.

ACKNOWLEDGMENT

We acknowledge support of this research from the National Science Foundation (CBET-1803409 and EFMA-1935252), and the Army Research Office through W911NF-15-1-0568 and W911NF-17-1-0575. The authors also thank Soumita Maiti for helpful comments on this work.

REFERENCES

(1) Peaudecerf, F. J.; Landel, J. R.; Goldstein, R. E.; Luzzatto-Fegiz, P. Traces of Surfactants Can Severely Limit the Drag Reduction of Superhydrophobic Surfaces. *Proc. Natl. Acad. Sci. U. S. A.* **2017**, *114*, 7254–7259.

(2) Langevin, D. Rheology of Adsorbed Surfactant Monolayers at Fluid Surfaces. *Annu. Rev. Fluid Mech.* **2014**, *46*, 47–65.

(3) Roché, M.; Li, Z.; Griffiths, I. M.; Le Roux, S.; Cantat, I.; Saint-Jalmes, A.; Stone, H. A. Marangoni Flow of Soluble Amphiphiles. *Phys. Rev. Lett.* **2014**, *112*, 208302.

(4) Quéré, D. Fluid Coating on a Fiber. *Annu. Rev. Fluid Mech.* **1999**, *31*, 347–384.

(5) Datwani, S. S.; Truskett, V. N.; Rosslee, C. A.; Abbott, N. L.; Stebe, K. J. Redox-Dependent Surface Tension and Surface Phase Transitions of a Ferrocenyl Surfactant: Equilibrium and Dynamic Analyses with Fluorescence Images. *Langmuir* **2003**, *19*, 8292–8301.

(6) Eggleton, C. D.; Tsai, T. M.; Stebe, K. J. Tip Streaming from a Drop in the Presence of Surfactants. *Phys. Rev. Lett.* **2001**, *87*, 48302.

(7) Anna, S. L. Droplets and Bubbles in Microfluidic Devices. *Annu. Rev. Fluid Mech.* **2016**, *48*, 285–309.

(8) Moyle, T. M.; Walker, L. M.; Anna, S. L. Predicting Conditions for Microscale Surfactant Mediated Tipstreaming. *Phys. Fluids* **2012**, *24*, 082110.

(9) Chen, C. V. H. H.; Liu, Y.; Stone, H. A.; Prud'Homme, R. K. Visualization of Surfactant Dynamics to and along Oil-Water Interfaces Using Solvatochromic Fluorescent Surfactants. *Langmuir* **2018**, *34*, 10512–10522.

(10) Alvarez, N. J.; Vogus, D. R.; Walker, L. M.; Anna, S. L. Using Bulk Convection in a Microtensiometer to Approach Kinetic-Limited Surfactant Dynamics at Fluid-Fluid Interfaces. *J. Colloid Interface Sci.* **2012**, *372*, 183–191.

(11) Stebe, K. J.; Maldarelli, C. Remobilizing Surfactant Retarded Fluid Particle Interfaces. II. Controlling the Surface Mobility at Interfaces of Solutions Containing Surface Active

Components. *J. Colloid Interface Sci.* **1994**, *163*, 177–189.

(12) Manikantan, H.; Squires, T. M. Surfactant Dynamics: Hidden Variables Controlling Fluid Flows. *J. Fluid Mech.* **2020**, *892*, 1–115.

(13) Hu, H.; Larson, R. G. Analysis of the Effects of Marangoni Stresses on the Microflow in an Evaporating Sessile Droplet. *Langmuir* **2005**, *21*, 3972–3980.

(14) Chen, J.; Stebe, K. J. Marangoni Retardation of the Terminal Velocity of a Settling Droplet: The Role of Surfactant Physico-Chemistry. *J. Colloid Interface Sci.* **1996**, *178*, 144–155.

(15) He, Y.; Yazhgur, P.; Salonen, A.; Langevin, D. Adsorption-Desorption Kinetics of Surfactants at Liquid Surfaces. *Adv. Colloid Interface Sci.* **2015**, *222*, 377–384.

(16) Eastoe, J.; Rankin, A.; Wat, R.; Bain, C. D.; Styrkas, D.; Penfold, J. Dynamic Surface Excesses of Fluorocarbon Surfactants. *Langmuir* **2003**, *19*, 7734–7739.

(17) Kirby, S. M.; Anna, S. L.; Walker, L. M. Sequential Adsorption of an Irreversibly Adsorbed Nonionic Surfactant and an Anionic Surfactant at an Oil/Aqueous Interface. *Langmuir* **2015**, *31*, 4063–4071.

(18) Stebe, K. J.; Lin, S. Y.; Maldarelli, C. Remobilizing Surfactant Retarded Fluid Particle Interfaces. I. Stress-Free Conditions at the Interfaces of Micellar Solutions of Surfactants with Fast Sorption Kinetics. *Phys. Fluids A* **1991**, *3*, 3–20.

(19) Brake, J. M.; Daschner, M. K.; Luk, Y.; Abbott, N. L. Biomolecular Interactions at Phospholipid-Decorated Surfaces of Liquid Crystals. *Science* **2003**, *302*, 2094–2097.

(20) Gupta, J. K.; Meli, M. V.; Teren, S.; Abbott, N. L. Elastic Energy-Driven Phase Separation

of Phospholipid Monolayers at the Nematic Liquid-Crystal-Aqueous Interface. *Phys. Rev. Lett.* **2008**, *100*, 048301.

(21) Dunér, G.; Kim, M.; Tilton, R. D.; Garoff, S.; Przybycien, T. M. Effect of Polyelectrolyte-Surfactant Complexation on Marangoni Transport at a Liquid-Liquid Interface. *J. Colloid Interface Sci.* **2016**, *467*, 105–114.

(22) de Gennes, P. G.; Prost, J. *The Physics of Liquid Crystals*, 2nd ed.; Clarendon Press, 1993.

(23) Kleman, M.; Lavrentovich, O. D. *Soft Matter Physics: An Introducion*, 1st ed.; Springer, 2003.

(24) Miller, D. S.; Carlton, R. J.; Mushenheim, P. C.; Abbott, N. L. Instructional Review: An Introduction to Optical Methods for Characterizing Liquid Crystals at Interfaces. *Langmuir* **2013**, *29*, 3154–3169.

(25) Tsuei, M.; Shivrayan, M.; Kim, Y.-K.; Thayumanavan, S.; Abbott, N. L. Optical "Blinking" Triggered by Collisions of Single Supramolecular Assemblies of Amphiphilic Molecules with Interfaces of Liquid Crystals. *J. Am. Chem. Soc.* **2020**, *142*, 6139–6148.

(26) Kim, Y. K.; Huang, Y.; Tsuei, M.; Wang, X.; Gianneschi, N. C.; Abbott, N. L. Multi-Scale Responses of Liquid Crystals Triggered by Interfacial Assemblies of Cleavable Homopolymers. *ChemPhysChem* **2018**, *19*, 2037–2045.

(27) Gelebart, A. H.; Jan Mulder, D.; Varga, M.; Konya, A.; Vantomme, G.; Meijer, E. W.; Selinger, R. L. B.; Broer, D. J. Making Waves in a Photoactive Polymer Film. *Nature* **2017**, *546*, 632–636.

(28) Adamiak, L.; Pendery, J.; Sun, J.; Iwabata, K.; Gianneschi, N. C.; Abbott, N. L. Design Principles for Triggerable Polymeric Amphiphiles with Mesogenic Side Chains for Multiscale Responses with Liquid Crystals. *Macromolecules* **2018**, *51*, 1978–1985.

(29) Zhou, J.; Dong, Y.; Zhang, Y.; Liu, D.; Yang, Z. The Assembly of DNA Amphiphiles at Liquid Crystal-Aqueous Interface. *Nanomaterials* **2016**, *6*, 229.

(30) Wang, X.; Yang, P.; Mondiot, F.; Li, Y.; Miller, D. S.; Chen, Z.; Abbott, N. L. Interfacial Ordering of Thermotropic Liquid Crystals Triggered by the Secondary Structures of Oligopeptides. *Chem. Commun.* **2015**, *51*, 16844–16847.

(31) Carlton, R. J.; Ma, C. D.; Gupta, J. K.; Abbott, N. L. Influence of Specific Anions on the Orientational Ordering of Thermotropic Liquid Crystals at Aqueous Interfaces. *Langmuir* **2012**, *28*, 12796–12805.

(32) Carlton, R. J.; Gupta, J. K.; Swift, C. L.; Abbott, N. L. Influence of Simple Electrolytes on the Orientational Ordering of Thermotropic Liquid Crystals at Aqueous Interfaces. *Langmuir* **2012**, *28*, 31–36.

(33) Tang, X.; Selinger, J. V. Minimization Principle for Shear Alignment of Liquid Crystals. *Phys. Rev. E* **2020**, *101*, 032701.

(34) Buttsworth, D. R.; Elston, S. J.; Jones, T. V. Direct Full Surface Skin Friction Measurement Using Nematic Liquid Crystal Techniques. *J. Turbomach.* **1997**, *4*, 847–853.

(35) Archer, L. A.; Larson, R. G. A Molecular Theory of Flow Alignment and Tumbling in Sheared Nematic Liquid Crystals. *J. Chem. Phys.* **1995**, *103*, 3108–3111.

(36) Itoh, S.; Imura, Y.; Fukuzawa, K.; Zhang, H. Anisotropic Shear Viscosity of Photoaligned Liquid Crystal Confined in Submicrometer-to-Nanometer-Scale Gap Widths Revealed with Simultaneously Measured Molecular Orientation. *Langmuir* **2015**, *31*, 11360–11369.

(37) Rey, A. D. Thermodynamics of Soft Anisotropic Interfaces. *J. Chem. Phys.* **2004**, *120*, 2010–2019.

(38) Rey, A. D. Mechanics of Soft-Solid-Liquid-Crystal Interfaces. *Phys. Rev. E* **2005**, *72*, 011706.

(39) Rey, A. D. Tension Gradients and Marangoni Flows in Nematic Interfaces. *Phys. Rev. E - Stat. Physics, Plasmas, Fluids, Relat. Interdiscip. Top.* **1999**, *60*, 1077–1080.

(40) Rey, A. D. Marangoni Flow in Liquid Crystal Interfaces. *J. Chem. Phys.* **1999**, *110*, 9769–9770.

(41) Kim, Y.; Wang, X.; Mondkar, P.; Bukusoglu, E.; Abbott, N. L. Self-Reporting and Self-Regulating Liquid Crystals. *Nature* **2018**, *557*, 539–544.

(42) Krüger, C.; Bahr, C.; Herminghaus, S.; Maass, C. C. Dimensionality Matters in the Collective Behaviour of Active Emulsions. *Eur. Phys. J. E* **2016**, *39*, 64.

(43) Maass, C. C.; Krüger, C.; Herminghaus, S.; Bahr, C. Swimming Droplets. *Annu. Rev. Condens. Matter Phys.* **2016**, *7*, 171–193.

(44) Herminghaus, S.; Maass, C. C.; Krüger, C.; Thutupalli, S.; Goehring, L.; Bahr, C. Interfacial Mechanisms in Active Emulsions. *Soft Matter* **2014**, *10*, 7008–7022.

(45) Peddireddy, K.; Kumar, P.; Thutupalli, S.; Herminghaus, S.; Bahr, C. Solubilization of

Thermotropic Liquid Crystal Compounds in Aqueous Surfactant Solutions. *Langmuir* **2012**, *28*, 12426–12431.

(46) Hokmabad, B. V.; Baldwin, K. A.; Krüger, C.; Bahr, C.; Maass, C. C. Topological Stabilization and Dynamics of Self-Propelling Nematic Shells. *Phys. Rev. Lett.* **2019**, *123*, 178003.

(47) Yang, Z.; Abbott, N. L. Spontaneous Formation of Water Droplets at Oil-Solid Interfaces. *Langmuir* **2010**, *26*, 13797–13804.

(48) Kim, Y. K.; Raghupathi, K. R.; Pendery, J. S.; Khomein, P.; Sridhar, U.; de Pablo, J. J.; Thayumanavan, S.; Abbott, N. L. Oligomers as Triggers for Responsive Liquid Crystals. *Langmuir* **2018**, *34*, 10092–10101.

(49) Brake, J. M.; Abbott, N. L. An Experimental System for Imaging the Reversible Adsorption of Amphiphiles at Aqueous-Liquid Crystal Interfaces. *Langmuir* **2002**, *18*, 6101–6109.

(50) Patrício, P.; Leal, C. R.; Pinto, L. F. V.; Boto, A.; Ciadade, M. . Electro-Rheology Study of a Series of Liquid Crystal Cyanobiphenyls: Experimental and Theoretical Treatment. *Liq. Cryst.* **2012**, *39*, 25–37.

(51) Chen, H.; Gao, Y.; Stone, H. A.; Li, J. “Fluid Bearing” Effect of Enclosed Liquids in Grooves on Drag Reduction in Microchannels. *Phys. Rev. Fluids* **2016**, *1*, 083904.

(52) Pan, F.; Acrivos, A. Steady Flows in Rectangular Cavities. *J. Fluid Mech.* **1967**, *28*, 643–655.

(53) Bonfillon, A.; Sicoli, F.; Langevin, D. Dynamic Surface Tension of Ionic Surfactant

Solutions. 1994, pp 497–504.

(54) Buka, A.; Kramer, L. *Pattern Formation in Liquid Crystals*, 1st ed.; Springer, 1996.

(55) Luskin, M.; Pan, T. W. Non-Planar Shear Flows for Non-Aligning Nematic Liquid Crystals. *J. Nonnewton. Fluid Mech.* **1992**, *42*, 369–384.

(56) Yesil, F.; Suwa, M.; Tsukahara, S. Anchoring Energy Measurements at the Aqueous Phase/Liquid Crystal Interface with Cationic Surfactants Using Magnetic Fréedericksz Transition. *Langmuir* **2018**, *34*, 81–87.

(57) Shioi, A.; Nagaoka, R.; Sugiura, Y. Desorption of Ionic-Surfactants at Liquid/Liquid Interface. *J. Chem. Eng. Japan* **2000**, *33*, 679–683.

(58) Pinazo, A.; Wen, X.; Liao, Y. C.; Prosser, A. J.; Franses, E. I. Comparison of DLPC and DPPC in Controlling the Dynamic Adsorption and Surface Tension of Their Aqueous Dispersions. *Langmuir* **2002**, *18*, 8888–8896.

(59) Gupta, J. K.; Abbott, N. L. Principles for Manipulation of the Lateral Organization of Aqueous-Soluble Surface-Active Molecules at the Liquid Crystal-Aqueous Interface. *Langmuir* **2009**, *25*, 2026–2033.

(60) Liu, J.; Radja, A.; Gao, Y.; Yin, R.; Sweeney, A.; Yang, S. Mimicry of a Biophysical Pathway Leads to Diverse Pollen-like Surface Patterns. *Proc. Natl. Acad. Sci. U. S. A.* **2020**, *117*, 9699–9705.

(61) Brake, J. M.; Mezera, A. D.; Abbott, N. L. Effect of Surfactant Structure on the Orientation of Liquid Crystals at Aqueous-Liquid Crystal Interfaces. *Langmuir* **2003**, *19*, 6436–6442.

(62) Brake, J. M.; Abbott, N. L. Coupling of the Orientations of Thermotropic Liquid Crystals to Protein Binding Events at Lipid-Decorated Interfaces. *Langmuir* **2007**, *23*, 8497–8507.

Table of Contents